

FLUIDIZED-BED PYROLYSIS OF OIL SHALE

J. H. Richardson and E. B. Huss
Chemistry and Materials Science Department
Lawrence Livermore National Laboratory
Livermore, CA 94550

Abstract

Several quartz isothermal fluidized-bed reactors have been constructed in order to measure kinetics and oil properties relevant to surface retorting by fluidized-bed processes. The rate of volatile total hydrocarbon evolution is measured with a flame ionization detector, although various techniques are currently being evaluated for doing species-selective (as opposed to total hydrocarbon) kinetics. Oil yield experiments are performed separately from the kinetic experiments due to the experimental conditions necessary to minimize mist formation and maximize oil collection. Oil composition is determined via subsequent analysis (gas chromatography). Gas evolution kinetics, oil yield and oil composition are determined both as a function of oil shale parameters (e.g., particle size, grade, Eastern vs. Western deposits) and fluidized-bed parameters (temperature, sweep gas composition, gas velocity, bed particle size, and bed geometry). An ultimate goal is the development of diagnostic methods relating oil composition to processing parameters.

*Work performed under the auspices of the U. S. Department of Energy by the Lawrence Livermore National Laboratory under contract number W-7405-ENG-48.

7912o/10/81

INTRODUCTION

There is considerable commercial interest in aboveground oil shale retorting using fluidized-bed processing techniques.¹ Such techniques are characterized by rapid heating of the oil shale followed by essentially isothermal retorting with the subsequent rapid removal of the pyrolysis products. Recently a kinetic study by Wallman, et al. using one type of oil shale has been reported which is applicable to these processing techniques.² Their study indicated a particle size dependence for both the oil yield and the pyrolysis kinetics, where the particle size was varied between 0.4 and 3 mm. These results were interpreted with the aid of a two-step model for kerogen decomposition with each step following first-order kinetics. The initial kerogen decomposition rate constant varied from 1 to 10 min⁻¹ over a temperature range of 480-540°C; the rate constant for the second step varied from 0.1 to 1 min⁻¹ over the same temperature range. This second rate constant was associated with the decomposition of a heavy oil intermediate, which, along with a predominantly lighter hydrocarbon fraction, was the result of the initial kerogen decomposition step.

The purpose of our work is twofold: 1) to extend the kinetic studies of Wallman, et al.² to a variety of oil shales, thereby testing their general applicability; 2) to characterize the oil produced in a fluidized-bed reactor with the goal of developing diagnostic techniques similar to those previously determined for MIS retorting.^{3,4} In this paper we present both our preliminary kinetic results and our preliminary oil characterization results. Generally there is good agreement between our results and those of Wallman, et al.² for the initial kerogen decomposition step; however, we have not determined such a definite particle size dependence for the second decomposition step. Although preliminary, initial gas chromatograms of collected oil show a relatively high amount of isoprenoid compounds; observed 1-alkene/n-alkane ratios are consistent with those expected from extrapolated trends of data obtained at lower heating rates.

EXPERIMENTAL

Figure 1 is a schematic of the experimental apparatus. The fluid bed and condenser are quartz, connected with stainless steel unions and graphite

ferrules. The distributor is a multiorifice plate (seven hole grid design).

The bed itself consists of 100-150 g of sand (Baker), ground, sieved, and washed (-0.250 + 0.125 mm). To date only helium has been used as a fluidizing medium. Typical flow rates are 60-80 cc/s (NTP), corresponding to a superficial velocity in the fluid bed of about 13 cm/s at 500°C. This is approximately a factor of ten above the calculated minimum fluidization velocity,^{6,7} and the bed appears nicely fluidized (smooth fluidization⁷).

The heat source is a Lindberg three zone furnace. Typically the temperature in the sand is isothermal to $\pm 1^\circ\text{C}$. For the oil collection experiments, the temperature profile inside the quartz reactor is isothermal to $\pm 2^\circ\text{C}$ throughout the region heated by the furnace; outside the furnace, the temperature is maintained between 300-350°C with heating tape. Consequently, from the standpoint of gas-phase oil cracking losses, the mean residence time in the hotter fluid bed is approximately two seconds. For the kinetic experiments, the temperature refers only to that of the sand; the rest of the quartz fluid bed is cooler (e.g., when the sand was 560°C the temperature profile inside monotonically decreased to 450°C at the furnace exit).

A quartz capillary samples the pyrolysis products at a distance approximately 8 inches above the sand bed and nearly on the vertical axis through the fluid bed. A Varian flame ionization detector with Wilkens gas chromatograph electrometer is used to monitor the rate of hydrocarbon generation. Preliminary experiments demonstrated the need for a back pressure regulator at the system exit to ensure that the detector response was attributable solely to changes in hydrocarbon concentration and not pressure fluctuations. The FID response is calibrated with primary standards of methane in helium. The maximum detector response at 560°C to a typical 50 mg oil shale sample is comparable to that obtained with a 1% methane/helium mixture. The temporal response of the detection system was less than three seconds (10%-90%). Larger samples are used for the oil collection experiments (up to 5 g); although the larger sample does result in an initial temperature drop, the sand temperature is still constant to $\pm 2^\circ\text{C}$ during the course of the oil generation.

The FID results are digitized and manipulated using an HP1000 computer system. Currently most of the kinetic data is treated with a five-point smoothing routine and then by linear regression analysis, although programs for further smoothing the raw data and expressing the data in integral form are being developed.

The oil is collected in a condenser similar in design to that used by Wallman, et al.² Fines are excluded from the condenser by quartz wool and a quartz frit. The ice bath is maintained at 0°C ($\pm 2^\circ\text{C}$); currently no effort has been made to collect the non-condensables. All chromatography of the oil was done with a HP5880 gas chromatograph with data acquisition and subsequent data reduction using an HP1000 computer system; the procedures have been previously described.⁵

Table I summarizes the assays of the five oil shales used in this study; three of the samples are Western shales from the Piceance Basin (RB 432, RB 560, and Anvil Points) and two samples are Eastern shales from Lewis County, Kentucky (Sunbury shales CLE-002 and SUN-002). The oil yields for the Western shales are estimated from previously published correlations with percent organic carbon;⁸⁻¹⁰ the average of the three correlations is listed.

RESULTS AND DISCUSSION

Kinetics

In general the FID kinetic data is currently analyzed by first taking the \ln of the normalized response and then fitting by linear regression analysis to the form,

$$\ln(\text{rate}) = -k_1 t + A_1 \quad (1)$$

for short times ($0 \leq t \leq \tau$) and to the form

$$\ln(\text{rate}) = -k_2 t + A_2 \quad (2)$$

for long times ($t > \tau$), where τ is empirically determined by inspection. The directly determined value for k_1 is reported without correction for k_2 .

Figure 2 illustrated a typical kinetic result, plotting the \ln of the normalized FID response versus time for RB 432 and two different particle sizes. Figure 3 illustrates similar data for a leaner shale, RB 560. In the latter case there is little motivation to empirically fit more than one line to the data. However, with both RB 432 and Anvil Points shale two line segments were used to fit the data over an experimental time interval corresponding to a relative reduction in the rate of hydrocarbon generation by nearly two orders of magnitude. In all cases, the square of the correlation coefficient for the first line segment was greater than 0.93 and usually it was greater than 0.97; the second line segment had a somewhat lower correlation coefficient (r^2 ranging from .90 to .98) corresponding to more noise at the lower signal level. Further digital smoothing of the data and/or larger sample sizes may improve the linear correlation at low rates.

Figure 4 illustrates typical data used for an Arrhenius plot. In all cases, irrespective of particle size, the Western shales exhibited a similar dependence of k_1 on temperature; a similar dependence of k_2 on temperature was observed with RB 432 and Anvil Points. The Eastern shales had a significantly different rate of kerogen decomposition (Figure 5).

Figures 6-9 are Arrhenius plots comparing our results with those of Wallman, et al.² Figure 6 compares the value of k_1 determined for similarly sized particles from four different oil shales; Figure 7 does the same thing for the value of k_2 . Two conclusions are apparent: 1) the difference in retorting rate between Western and Eastern Oil shale is attributable to differences in k_1 ; 2) there is approximately a factor of five difference in the rate between Chevron's k_2 and ours (irrespective of oil shale source). Figures 8 and 9 compare the effect of particle size on k_1 and k_2 , respectively, for both Western and Eastern oil shale. There is none.

Table II summarizes the kinetic parameters determined in this work and compares them to the values previously reported. The calculated value of k_1 for Western shale at 500°C using our values is very similar to that calculated using the results of Wallman, et al.² (2.81 min⁻¹ vs. 2.72 min⁻¹, respectively). It is seen that the preexponential A factor is the major difference between the two expressions for k_2 ; the activation energies are

reasonably similar. In the case of the Eastern shale, the lower preexponential A factor is consistent with the general description of Eastern shale being more "coal-like" than Western shale (i.e., a lower H/C ratio), although several other factors are also likely to influence the A factor.

Agreement between our values for k_1 with Western shales and those of Wallman, et al.² is encouraging; conversely, the disagreement between the values for k_2 suggests further experiments are necessary. In general, our rate data exhibits considerable fluctuations from sample to sample at relatively low rates (less than 5% of the maximum); probably we would have better data (and better linear correlations) with larger and therefore more homogeneous samples (with further digital smoothing and/or integration). At this stage, we do not feel that a two-step sequential mechanism is unequivocally indicated for all oil shales by the phenomenological fitting of most of our data with two rate constants. Furthermore, we would be reluctant at this point to interpret the variation in E and A for the various rate constants in terms of a mechanistic model. More detailed kinetic studies, including species selective monitoring by either mass spectroscopy or Raman techniques, is currently being evaluated.

Oil Characterization

Oil collection currently has not been optimized. We are now consistently collecting only $95 \pm 5\%$ of the expected Fischer assay yield (of oil and water). A higher rod temperature (350°C instead of 150°C) leading to a larger thermophoretic effect aids in oil collection as does increasing the surface area (glass wool instead of glass beads). Larger sample aliquots for a given mass, as opposed to more but smaller aliquots totaling the same mass, also leads to larger collection efficiencies. All three of these observations are consistent with maximizing mist collection and minimizing mist formation.¹¹ Gas chromatographic analysis suggests that the lighter ends are still not being collected efficiently. Current problems with the precision and reproducibility of oil collection preclude making any inferences as to the effect of particle size on oil yield from various shales. Previously published results did demonstrate oil yields from smaller particles which slightly exceeded Fischer assay results (e.g., up to 109% Fischer assay at 427°C for 0.4 mm particles).²

Two representative gas chromatograms of oil retorted in the fluidized-bed apparatus are shown in Figure 10. The identification of isoprenoid compounds, indicated by I₁ and listed in Table III, is taken from reference 5.

Three observations can be readily made from Figure 10. First, the relatively high 1-alkene/n-alkane ratio is qualitatively consistent with a high heating rate, and the higher pyrolysis temperature consistently gives a higher ratio (Figure 11). Extrapolation of 1-alkene/n-alkane ratio data obtained⁵ at much lower heating rates (10^{-2} to 10^1 °C/min) to the present ratio indicates a heating rate (10^3 to 10^4 °C/min) consistent with the present experiment. Experimentally, we observe an FID response approximately seven seconds after the shale is dropped into the fluid bed; this implies a heating period of approximately 4 to 5 sec, or 10^3 to 10^4 °C/min.

For comparison, Figure 11 also shows the 1-alkene/n-alkane ratio for two other oils generated from different oil shales, TOSS #3-3 and LETC R-14. TOSS #3-3 was generated from a leaner sample of RB 432 under pseudo-Fischer assay conditions with an external sweep gas, and LETC R-14 was a simulated MIS retort with an even lower heating rate.

In addition to the higher alkene/alkane ratios for oil retorted in the fluidized-bed, Figure 11 also illustrates the pronounced even-odd trend in the ratios. This trend has been previously observed.^{5,12,13} The explanation is not well understood but probably relates to both the structure of kerogen and undoubtedly to the pyrolysis conditions; consequently, such a pronounced even-odd trend may have potential as a process diagnostic.

Secondly, the ratio of the sum of certain isoprenoid alkenes plus alkanes to the sum of normal alkenes plus alkanes has been shown to be largely independent of heating rate for modest heating rates.⁵ That trend appears to hold for the higher heating rates present in the fluidized-bed. Obviously, ratios which are a function of heating rate are more useful as potential diagnostics of oil processing conditions.

Thirdly, the predominance of prist-1-ene in the gas chromatograms is particularly striking. For example, the ratio of prist-1-ene to the sum of the C₁₇ and C₁₈ normal alkanes plus alkenes is 0.45, 0.66, 0.16, and

0.09 for fluidized-bed 462°C, fluidized bed 524°C, TOSS #3-3 and LETC R-14, respectively. These results indicate the potential application of a ratio based on prist-1-ene as a diagnostic to oil processing conditions. Furthermore, several major species, currently unidentified, are present in the gas chromatogram of oil generated in the fluidized-bed which are not present to a significant extent in oils generated under different retorting conditions. Further work is needed to characterize these compounds.

ACKNOWLEDGEMENTS

We would like to thank M. O. Bishop and J. R. Taylor for the construction of the apparatus, J. E. Clarkson and V. L. Duval for the gas chromatographic analysis, and L. L. Ott for assistance with the kinetic data reduction.

DISCLAIMER

This document was prepared as an account of work sponsored by an agency of the United States Government. Neither the United States Government nor the University of California nor any of their employees, makes any warranty, express or implied, or assumes any legal liability or responsibility for the accuracy, completeness, or usefulness of any information, apparatus, product, or process disclosed, or represents that its use would not infringe privately owned rights. Reference herein to any specific commercial products, process, or service by trade name, trademark, manufacturer, or otherwise, does not necessarily constitute or imply its endorsement, recommendation, or favoring by the United States Government or the University of California. The views and opinions of authors expressed herein do not necessarily state or reflect those of the United States Government thereof, and shall not be used for advertising or product endorsement purposes.

REFERENCES

1. P. W. Tamm, C. A. Bertelsen, G. M. Handel, B. G. Spars, and P. H. Wallman, American Petroleum Institute 46th Midyear Refining Meeting, Chicago, IL (May, 1981).
2. P. H. Wallman, P. W. Tamm, and B. G. Spars, "Oil Shale, Tar Sands, and Related Materials," ACS Symposium Series 163, 93 (1981).
3. A. K. Burnham and J. E. Clarkson, 13th Oil Shale Symposium, Golden, CO (April, 1980), pp 269-278.
4. J. H. Raley, Fuel 59, 419 (1980).
5. A. K. Burnham, J. E. Clarkson, M. F. Singleton, C. M. Wong, and R. W. Crawford, Geochim. Cosmochim. Acta, submitted for publication (1981).
6. F. A. Zenz and D. F. Othmer, FLUIDIZATION AND FLUID-PARTICLE SYSTEMS, (Reinhold Publishing Corp., New York, NY, 1960) Chapter 7.
7. D. Kunii and O. Levenspiel, FLUIDIZATION ENGINEERING, (R. E. Krieger Publishing Co., Huntington, NY, 1977), Chapter 3.
8. E. W. Cook, Fuel 53, 16 (1974).
9. R. N. Heistand and H. B. Humphries, Anal. Chem. 48, 1192 (1976).
10. M. F. Singleton, G. J. Koskinas, A. K. Burnham, and J. H. Raley, manuscript in preparation (1981).
11. S. Goren, University of California (Berkeley), private communication.
12. A. K. Burnham and R. L. Ward, "Oil Shale, Tar Sands, and Related Materials," ACS Symposium Series 163, 79 (1981).
13. I. Klesment, J. Anal. Appl. Pyrol. 2, 63 (1980).

Table I. Assay parameters of oil shale used in this work.

Oil Shale	% Total C	% Org. C	% H	Gal/Ton
RB 432	22.7	18.4	1.33	41.3 ^a
RB 560	14.1	8.8	1.45	19.4 ^a
Anvil Points	15.2	10.4	2.49	23.0 ^a
CLE-002	14.1	14.1	1.69	14.0
SUN-002	13.9	13.9	1.65	14.2

^aCalculated from correlations in refs. 8-10.

Table II. Comparison of kinetic parameters.

	k_1		k_2	
	E, kcal/mole	A, s ⁻¹	E, kcal/mole	A, s ⁻¹
Western shale				
This work ^a	41.1	1.95×10^{10}	26.5 ^c	5.7×10^{5c}
Ref. 2	43.6	9.63×10^{10}	22.6	3.0×10^3
Eastern shale				
This work ^b	32.0	8.4×10^7	26.5 ^c	5.7×10^{5c}

^aIncludes data from RB 432 and Anvil Points.

^bData from CLE-002.

^cIncludes data from RB 432, Anvil Points, and CLE-002.

Table III. Identification of isoprenoid compounds labeled in Figure 10 (*tentative).

I2	2,6-dimethylundecane (C ₁₃)
I2'	2,6-dimethylundecene
I3	2,6,10-trimethylundecane (C ₁₄)
I3"	2,6,10-trimethylundec-2-ene*
I4	farnesane (C ₁₅)
I4'	farnesene
I5	2,6,10-trimethyltridecane (C ₁₆)
I5'	2,6,10-trimethyltridecene
I6	norpristane (C ₁₈)
I6'	norpristenes*
I7	pristane (C ₁₉)
I7'	prist-1-ene
I8	phytane (C ₂₀)

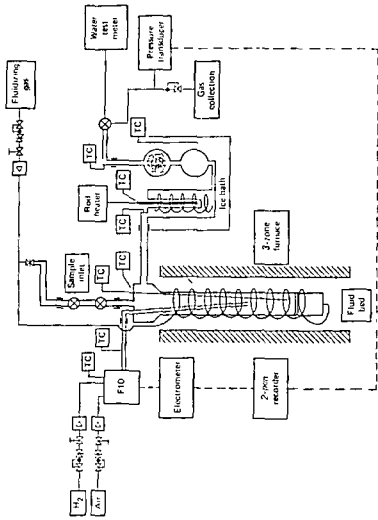


Figure 1. Schematic of the experimental apparatus for fluidized bed pyrolysis of oil shale.

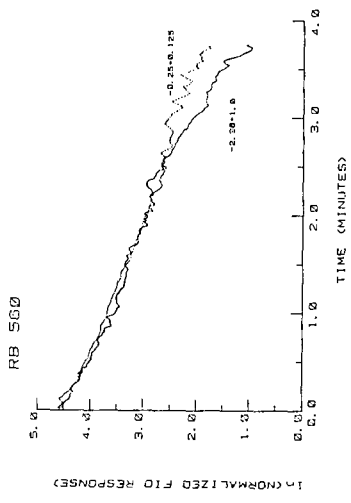


Figure 3. Typical kinetic results for RB 560 at 480°C. The ln of the normalized FID response is plotted vs. time for two particle sizes, -2.36 ± 1.0 mm and -0.25 ± 0.125 mm.

ANVIL POINTS -1.0+0.5

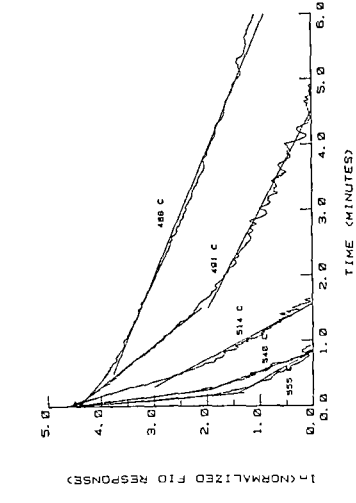


Figure 4. Typical kinetic results used to generate Arrhenius plot.

RB 432

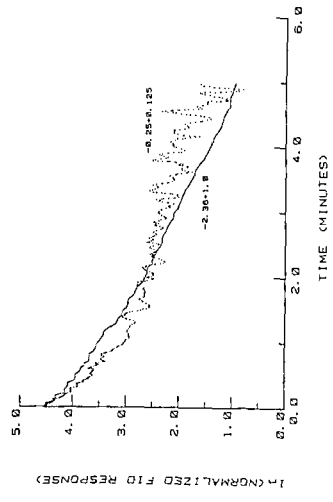


Figure 2. Typical kinetic results for RB 432 at 458°C. The ln of the normalized FID response is plotted vs. time for two particle sizes, -2.36 ± 1.0 mm and -0.25 ± 0.125 mm.

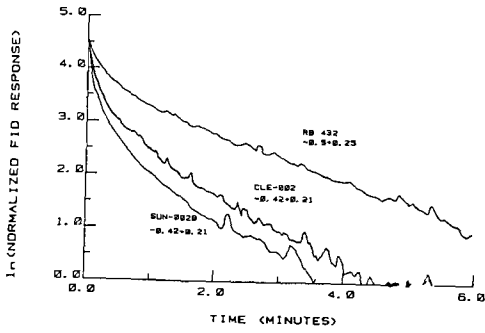


Figure 5. Comparison of kinetic results for Western vs. Eastern shales (466°C).

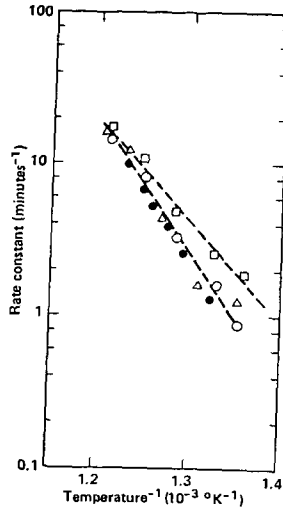


Figure 6. Arrhenius plot of k_1 , one particle size: (●) Chevron's results; (Δ) Anvil Points, -1.0 ± 0.5 mm; (○) RB 432, -1.0 ± 0.5 mm; (□) CLE-002, 1.0 ± 0.1 mm.

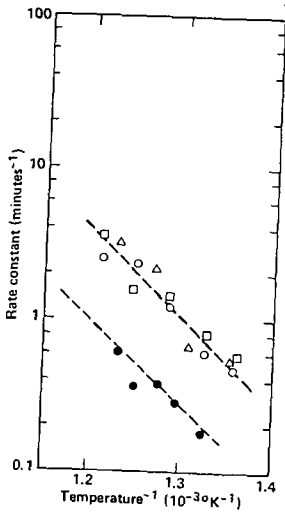


Figure 7. Arrhenius plot of k_2 , one particle size: (●) Chevron's results; (Δ) Anvil Points, -1.0 ± 0.5 mm; (○) RB 432, -1.0 ± 0.5 mm; (□) CLE-002, 1.0 ± 0.1 mm.

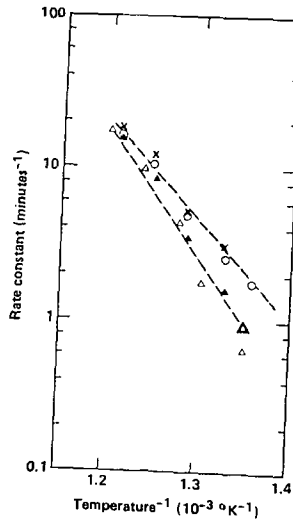


Figure 8. Arrhenius plot of k_3 , different particle sizes: (Δ) RB 432, -2.36 ± 1.0 mm; (○) RB 432, -1.0 ± 0.5 mm; (□) CLE-002, -1.0 ± 0.1 mm; (X) CLE-002, -0.42 ± 0.21 mm.

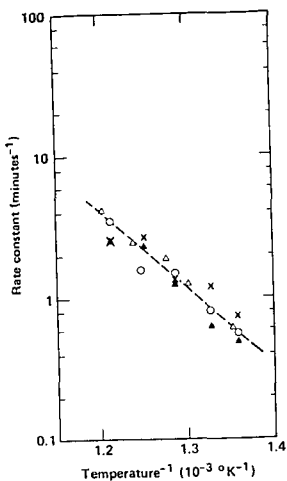


Figure 9. Arrhenius plot of k_p , different particle sizes: (Δ) RB 432, -2.36 ± 1.0 mm; (\bullet) RB 432, -1.0 ± 0.5 mm; (\circ) CLE-002, -1.0 ± 0.1 mm; (\times) CLE-002, -0.42 ± 0.21 mm.

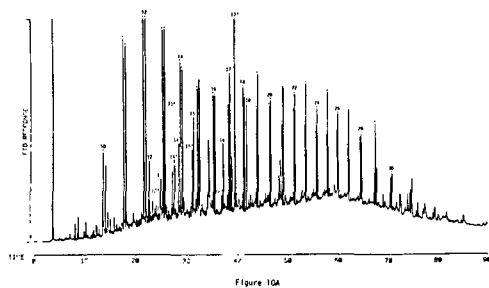


Figure 10A

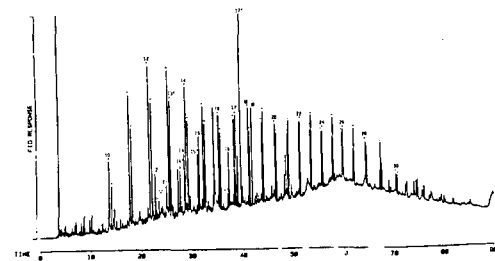


Figure 10. Gas chromatograms of oil reformed in the fluidized bed reactor. 1-alkanes and 1-alkenes are indicated by a dot, with the 1-alkene having the shorter retention time and even carbon numbers as indicated. Identified isoprenoid compounds are listed in Table II. A) 462°C; B) 52°C. Both oil shale samples were RB 432.

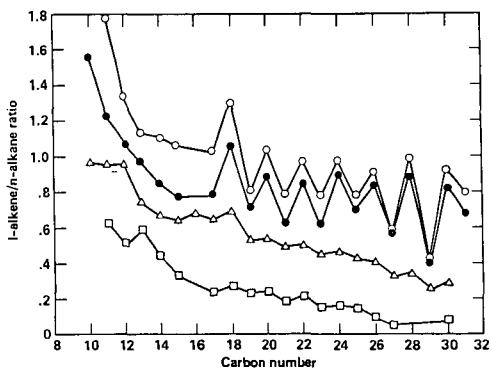


Figure 11. 1-alkene/n-alkane ratios for oils generated under different conditions: (\circ) RB 432 reformed in the fluidized bed, at 52°C; (\square) RB 432 reformed in the fluidized bed, at 462°C; (Δ) TOS 13-3, modest heating rate ($\sim 10^\circ\text{C}/\text{min}$), inert sweep gas; (\diamond) LFC R-14, simulated MIS.